Electronic Supplementary Information

for

An NAD^+-type earth-abundant metal complex enabling photo-driven alcohol oxidation

Hideki Ohtsu,*[a] Mikio Takaoka,[a] Yosuke Tezuka,[a] Kiyoshi Tsuge[a] and Koji Tanaka[b, c]

[a] *Graduate School of Science and Engineering, University of Toyama, 3190 Gofuku, Toyama 930-8555, Japan.*

[b] *Institute for Integrated Cell-Material Science, Institute for Advanced Study, Kyoto University, Yoshida-Ushinomiya-cho, Sakyo-ku, Kyoto 606-8501, Japan.*

[c] *Graduate School of Life Science, Ritsumeikan University, 1-1-1 Noji-Higashi, Kusatsu, Shiga 525-8577, Japan.*

*To whom correspondence should be addressed. E-mail: ohtsu@sci.u-toyama.ac.jp (H. Ohtsu)

Table of Contents

Experimental Details

Materials: All chemicals used for the synthesis of the ligands and complexes were commercial products of the highest available purity and were used without further purification unless otherwise noted. Solvents were purified by standard methods before use.[1] *Caution*: Perchlorate salts used herein are potentially explosive and must be handled with care and in small quantities.

Synthesis: All ligands and complexes used in this study were prepared according to the following procedures and the structures of the products were confirmed by the analytical data (*vide infra*).

pbn: This ligand used in this study was synthesised in accordance with the method of the literature.[2]

[Zn(pbn)$_2$(H$_2$O)](ClO$_4$)$_2$ (1): To a CH_2Cl_2 solution of pbn (60.1 mg, 0.234 mmol) was added $Zn(ClO_4)_2$•$6H_2O$ (43.4 mg, 0.117 mmol), and the mixture was stirred for 3 days at room temperature. The resulting powder was collected by filtration and recrystallized from CH_3CN/diethyl ether to afford colorless crystals of **1** (79.1 mg, 85.0%). ^{1}H NMR (300 MHz, CD_3CN, 20 ºC): δ 9.34 (2H, s), 9.24 (2H, d, J = 8.6 Hz), 9.02 (2H, d, J = 8.6 Hz), 8.92 (2H, d, J = 7.8 Hz), 8.44 (2H, t, J = 8.1 Hz), 8.37 (2H, d, J = 8.8 Hz), 8.33 (2H, d, J = 5.1 Hz), 8.12 (2H, d, J = 8.1 Hz), 8.05 (2H, ddd, J = 8.8, 6.6, 1.3 Hz), 7.75 (2H, t, J = 7.0 Hz), 7.62 (2H, dd, J = 7.5, 5.3 Hz) ppm. Anal. Calcd for $C_{34}H_{24}N_6O_9ZnCl_2$: C, 51.25%; H, 3.04%; N, 10.55%; Found: C, 51.32%; H, 3.33%; N, 10.57%. HR-ESI-MS: *m/z* Calcd for $C_{34}H_{22}N_6Zn$ $[M]^{2+}$: 289.0599; Found: 289.0600.

[Zn(pbnH–pbnH)(ClO$_4$)$_2$] (1^{red}): An CH_3CN solution (6 mL) of **1** (20.1 mg, 0.0252 mmol) containing 10% v/v 2-propanol was irradiated with light through a longpass filter (HOYA L37) and a super cold filter (ASAHI SPECTRA SC0751) using a 150 W Xenon lamp for 12 hours. Slow vapour diffusion of diethyl ether into the resulting solution was performed in the glove box under anaerobic conditions. Yellow crystals of **1^{red}** were obtained from the mixture solution after several weeks (13.4 mg, 68.0%). ^{1}H NMR (300 MHz, CD_3CN, 20 ºC): δ 8.57 (2H, m), 8.48 (2H, d, J = 8.3 Hz), 8.37–8.30 (4H, m), 8.15 (2H, s), 7.75 (2H, ddd, J = 7.2, 5.3, 1.2 Hz), 7.64 (2H, d, J = 8.8 Hz), 6.96 (2H, td, J = 7.6, 1.5 Hz), 6.74–6.70 (4H, m), 6.59 (2H, td, J = 7.4, 1.2 Hz), 5.42 (2H, s) ppm. Anal. Calcd for $C_{34}H_{24}N_6O_8ZnCl_2$: C, 52.30%; H, 3.10%; N, 10.76%; Found: C, 52.13%; H, 3.10%; N, 10.77%. HR-ESI-MS: *m/z* Calcd for $C_{34}H_{24}N_6Zn$ $[M]^{2+}$: 290.0677; Found: 290.0678.

Instrumentation and methods: NMR measurements were performed with a JEOL JMN-ECX 300 (300 MHz) NMR spectrometer. Elemental analyses were carried out using a Yanaco CHN Corder MT-5 (A Rabbit Science Japan Co., Ltd.). Absorption spectra were measured with a Hewlett-Packard 8453 diode array spectrophotometer. Emission spectra were recorded on a JASCO FP-8500 spectrofluorometer. ESI mass spectra were obtained with a Shimadzu LCMS-2020. High-resolution ESI mass spectra were recorded on a Thermo Fisher Scientific LTQ Orbitrap XL ETD. Cyclic voltammetry (CV) and second-harmonic alternating-current voltammetry (SHACV) measurements were performed on an ALS/Chi model 733D electrochemical analyzer in a deaerated solvent containing 0.1 M tetra-*n*-butylammonium hexafluorophosphate ($TBAPF_6$) as a supporting electrolyte. A conventional three-electrode cell was used with a glassy-carbon working electrode and a platinum wire as the counter electrode. The glassy-carbon working electrode was routinely polished with a BAS polishing alumina suspension and rinsed with acetone before use. All potentials were recorded against an Ag/Ag^+ (0.01 M $AgNO_3$/0.1 M $TBAPF_6$ in CH_3CN) reference electrode and were converted to values vs SCE by adding 0.29 V.[3] All electrochemical measurements were carried out under an argon atmosphere. The quantum yields of the photochemical aliphatic alcohol oxidation were determined using a Shimadzu absolute photoreaction quantum yields measurement system QYM-01 equipped with a 370 nm band-pass filter and a 300 W Xe lamp. Gas chromatography (GC) analyses were carried out on a Shimadzu GC-2014 gas chromatograph (He carrier) equipped with a flame ionization detector (FID) and a Stabilwax column. Gas chromatography mass spectrometry (GC−MS) data were obtained on a Shimadzu GCMS-QP2010 instrument (He carrier) equipped with a Stabilwax column. All reactions were run in an 1.0 cm quartz cuvette by monitoring UV-vis spectral changes of reaction solutions of **1** (0.05 mM) in the large excess of alcohols (0.50–3.0% v/v) in CH_3CN at 298 K using a 150 W Xe lamp (HAMAMATSU E7536) equipped with a longpass filter (HOYA L37) and a super cold filter (ASAHI SPECTRA SC0751) for irradiation. After the completion of reactions, pseudo-first-order fitting of the kinetic data allowed us to determine the pseudo-first-order rate constants. Products formed in the oxidation of the alcohols by **1** in CH_3CN at 298 K after rradiation of the light (370 nm~) were analyzed by injecting the reaction mixture directly into GC and GC−MS. Products were identified by comparison of the retention time and mass peaks of the products with respect to authentic samples, and product yields were determined by comparing the responsive peak areas of reaction products against standard curves prepared with known authentic samples.

X-ray crystal structure determination: The single crystal X-ray diffraction data of **1** and **1**^{red} were collected on a Rigaku VariMax RAPID-DW/NAT with Mo-*K*α radiation (λ = 0.71075 Å) at 173 K and processed using RapidAuto program (Rigaku). Their structures were solved by direct methods using SHELXT-2018/2[4] and refined by full-matrix least-squares techniques on F^2 using SHELXL-2018/3.[5] All non-hydrogen atoms were refined anisotropically and all hydrogen atoms were included in the refinement process as per the riding model.

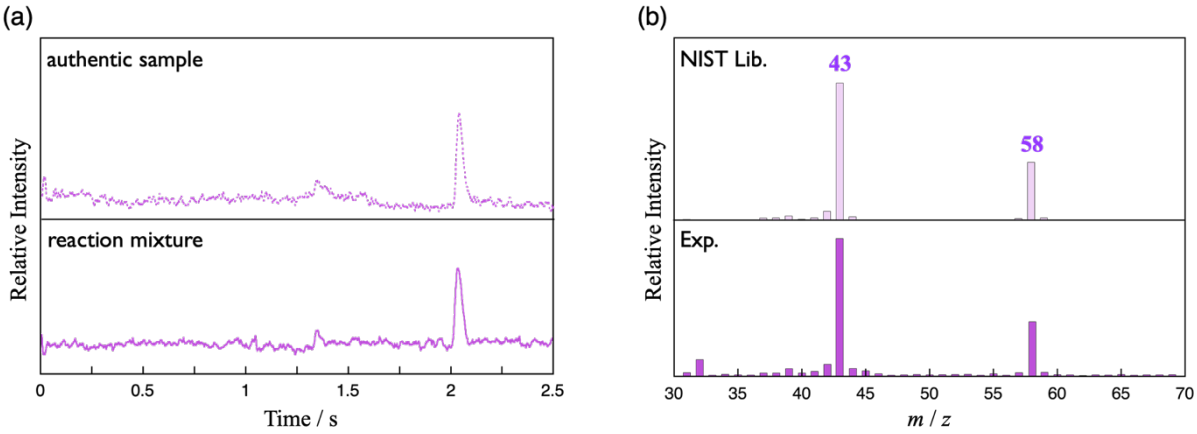

Fig. S1 (a) GC charts of reaction mixture after photoirradiation of the 0.05 mM CH_3CN solution of **1** containing 3.0% v/v 2-propanol with the light (370 nm~) for 1 h at 298 K (bottom) and an authentic sample of acetone (top). (b) GC−MS spectra of acetone produced by photoirradiation of the 0.05 mM CH_3CN solution of **1** containing 3.0% v/v 2-propanol with the light (370 nm~) for 1 h at 298 K (bottom) and fragmentation patterns of an authentic sample of acetone taken form the NIST mass spectral library (top).

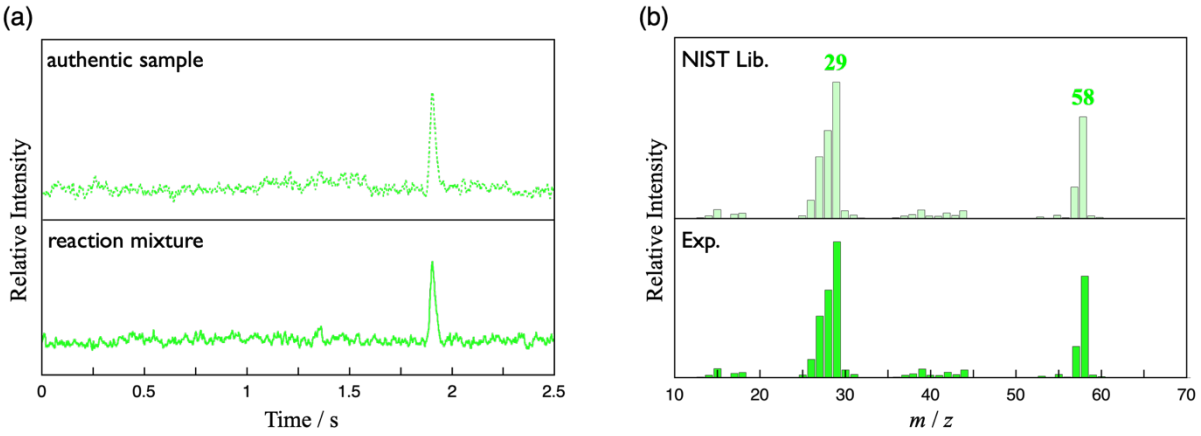

Fig. S2 (a) GC charts of reaction mixture after photoirradiation of the 0.05 mM CH_3CN solution of **1** containing 3.0% v/v 1-propanol with the light (370 nm~) for 1 h at 298 K (bottom) and an authentic sample of propionaldehyde (top). (b) GC−MS spectra of propionaldehyde produced by photoirradiation of the 0.05 mM CH_3CN solution of **1** containing 3.0% v/v 1-propanol with the light (370 nm~) for 1 h at 298 K (bottom) and fragmentation patterns of an authentic sample of propionaldehyde taken form the NIST mass spectral library (top).

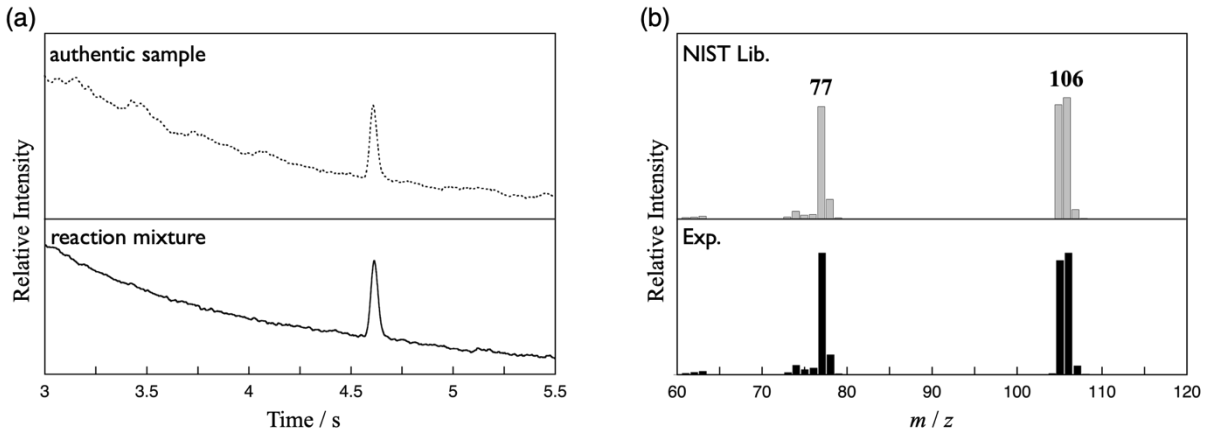

Fig. S3 (a) GC charts of reaction mixture after photoirradiation of the 0.05 mM CH_3CN solution of **1** containing 3.0% v/v benzyl alcohol with the light (370 nm~) for 1 h at 298 K (bottom) and an authentic sample of benzaldehyde (top). (b) GC−MS spectra of benzaldehyde produced by photoirradiation of the 0.05 mM CH_3CN solution of **1** containing 3.0% v/v benzyl alcohol with the light (370 nm~) for 1 h at 298 K (bottom) and fragmentation patterns of an authentic sample of benzaldehyde taken form the NIST mass spectral library (top).

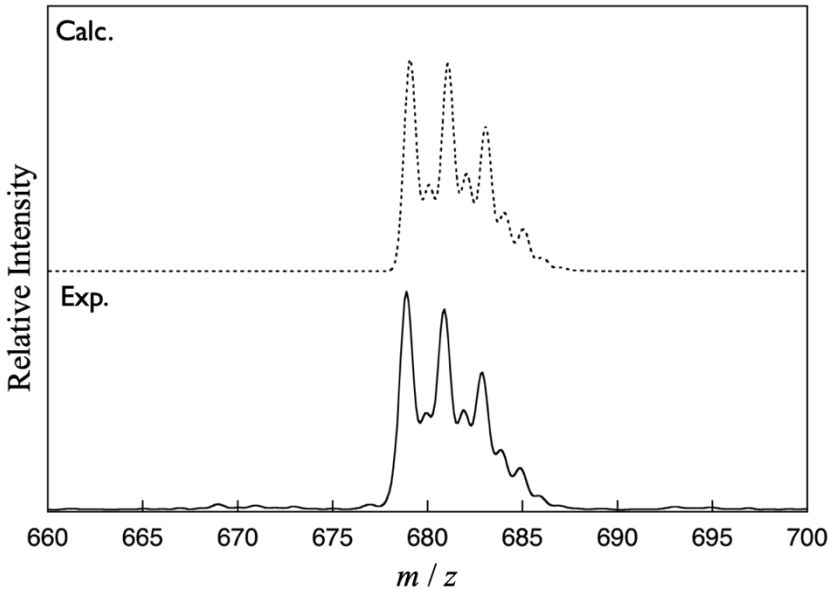

Fig. S4 Calculated (top) and observed (bottom) ESI mass spectra of $\mathbf{1}^{red}$ in CH_3CN at 298 K.

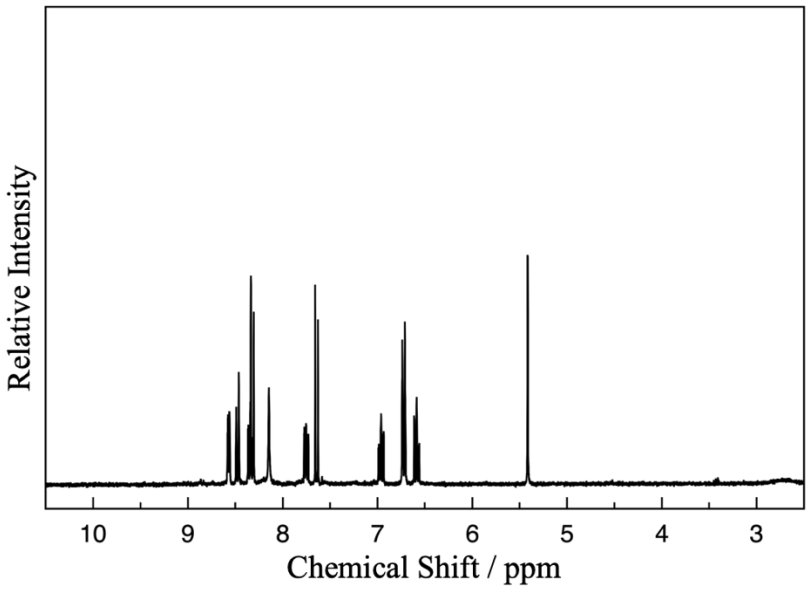

Fig. S5 ^{1}H NMR spectrum of $\mathbf{1}^{red}$ in CD_3CN at 293 K.

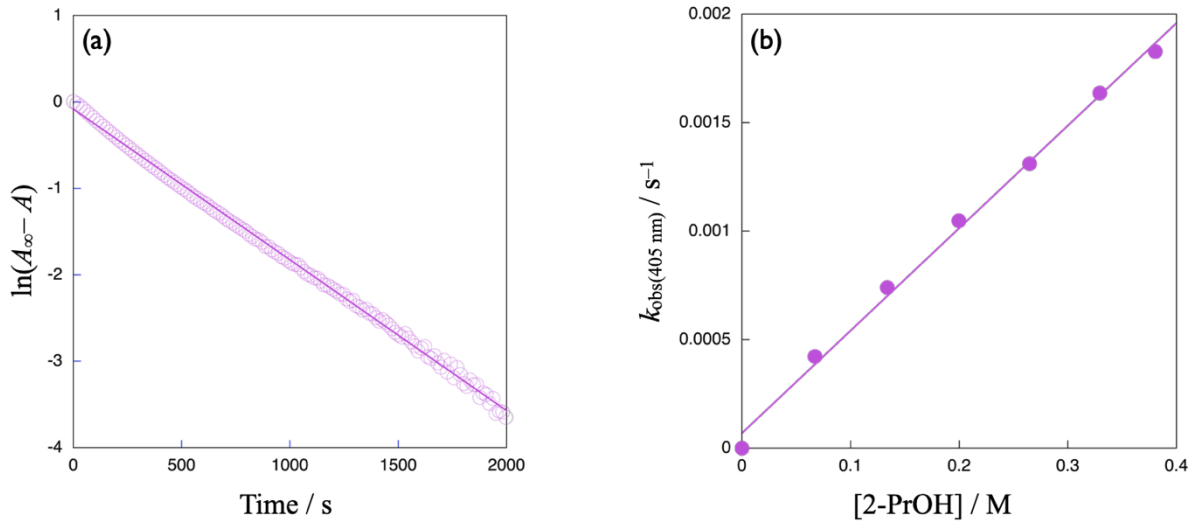

Fig. S6 (a) First-order plot based on the absorption change at 405 nm in the course of the photochemical oxidation of 2-propanol by **1** to produce $\mathbf{1}^{red}$ upon irradiation of the light (370 nm~) into the 0.05 mM CH_3CN solution of **1** in the presence of 3.0% v/v 2-propanol at 298 K. (b) Plot of the pseudo-first-order rate constant ($k_{obs(405nm)}$) versus concentration of 2-propanol for the photochemical oxidation of 2-propanol by **1** to produce $\mathbf{1}^{red}$.

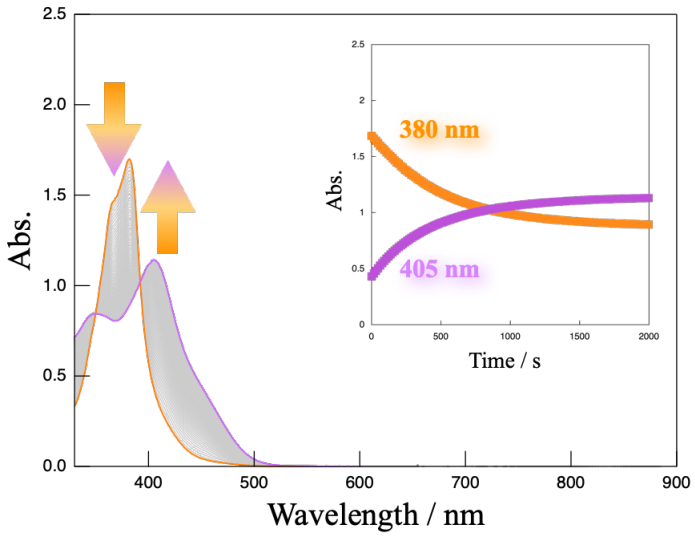

Fig. S7 Absorption spectral changes observed upon irradiation of the light (370 nm~) into the 0.05 mM CH_3CN solution of **1** in the presence of 3.0% v/v 2-propanol-d8 at 298 K. Inset: Time course of the absorption change at 380 nm (orange square) and 405 nm (purple square).

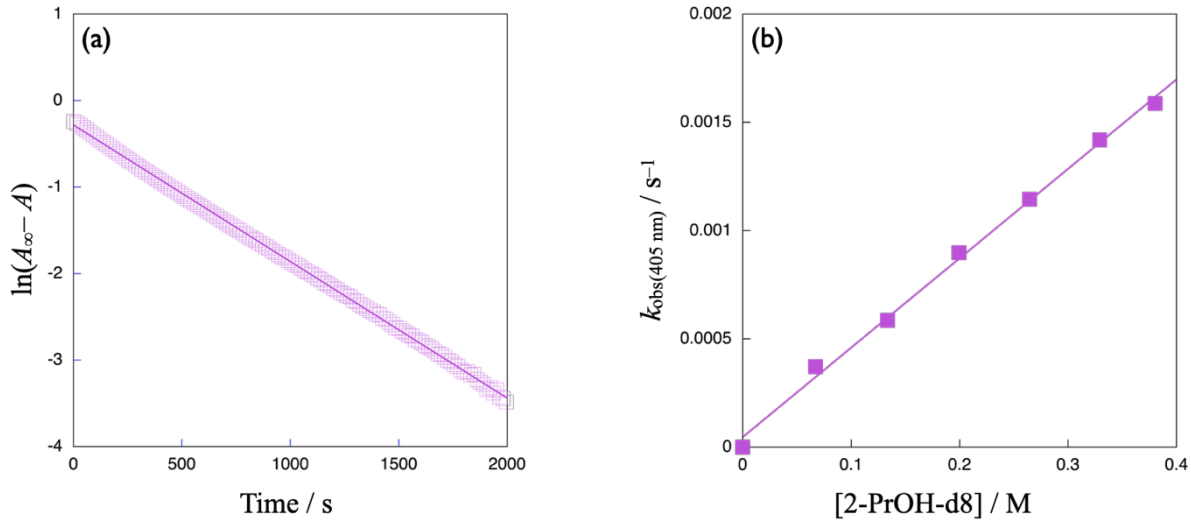

Fig. S8 (a) First-order plot based on the absorption change at 405 nm in the course of the photochemical oxidation of 2-propanol-d8 by **1** to produce $\mathbf{1}^{red}$ upon irradiation of the light (370 nm~) into the 0.05 mM CH_3CN solution of **1** in the presence of 3.0% v/v 2-propanol-d8 at 298 K. (b) Plot of the pseudo-first-order rate constant ($k_{obs(405nm)}$) versus concentration of 2-propanol-d8 for the photochemical oxidation of 2-propanol-d8 by **1** to produce $\mathbf{1}^{red}$.

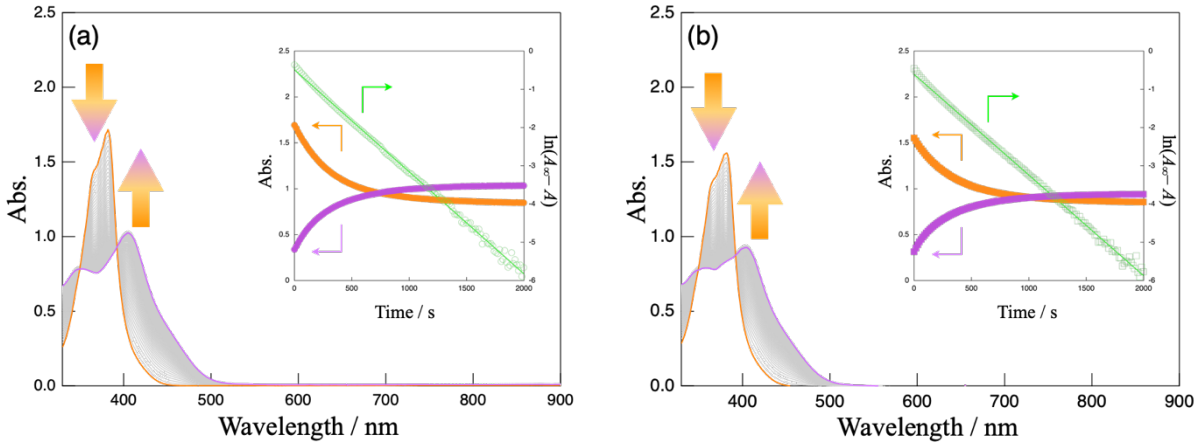

Fig. S9 Absorption spectral changes observed upon irradiation of the light (370 nm~) into the 0.05 mM CH_3CN solution of **1** in the presence of (a) 3.0% v/v 1-propanol and (b) 3.0% v/v 1-propanol-d8 at 298 K. Insets: (a) Time course of the absorption change at 380 nm (orange circle) and 405 nm (purple circle) and the first-order plots at 405 nm (green open circle). (b) Time course of the absorption change at 380 nm (orange square) and 405 nm (purple square) and the first-order plots at 405 nm (green open square).

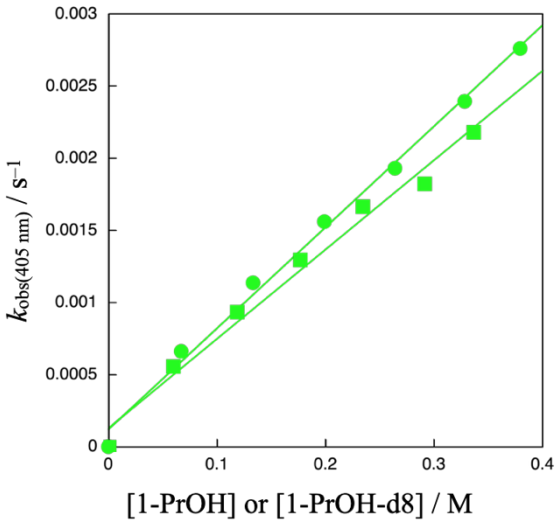

Fig. S10 Plots of the pseudo-first-order rate constant ($k_{obs(405nm)}$) versus concentration of 1-propanol (circle) or 1-propanol-d8 (square) for the photochemical oxidation of the alcohols by **1** to produce $\mathbf{1}^{red}$.

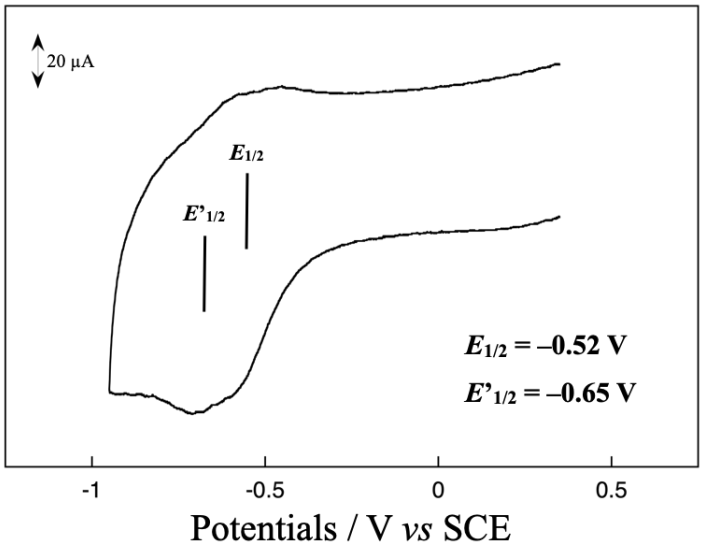

Fig. S11 Cyclic voltammogram of **1** in CH_3CN (1.0 mM) containing 0.1 M $TBAPF_6$ at 298 K (working electrode, glassy carbon; counter electrode, Pt wire; reference electrode, Ag/Ag^+; scan rate, 2.5 V s^{-1}).

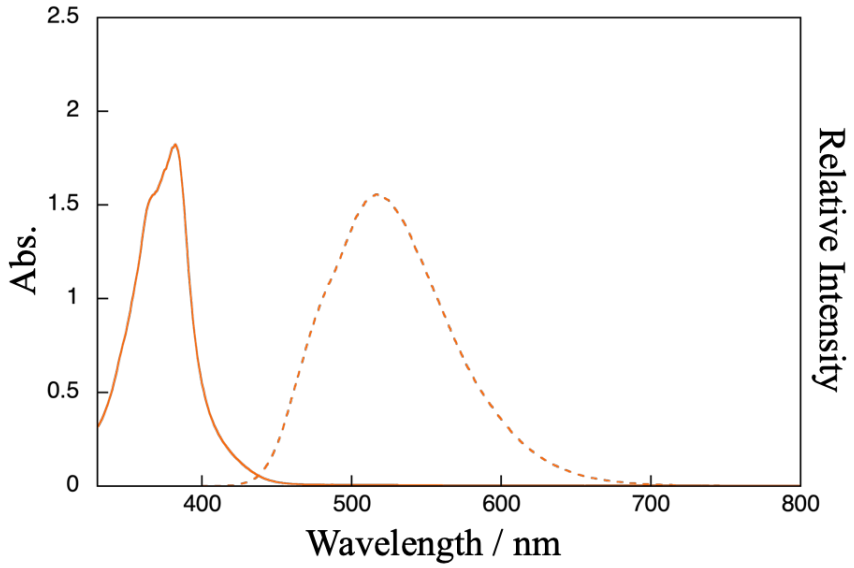

Fig. S12 Absorption (solid line) and emission (broken line) spectra of **1** in CH_3CN (0.05 mM) at 298 K.

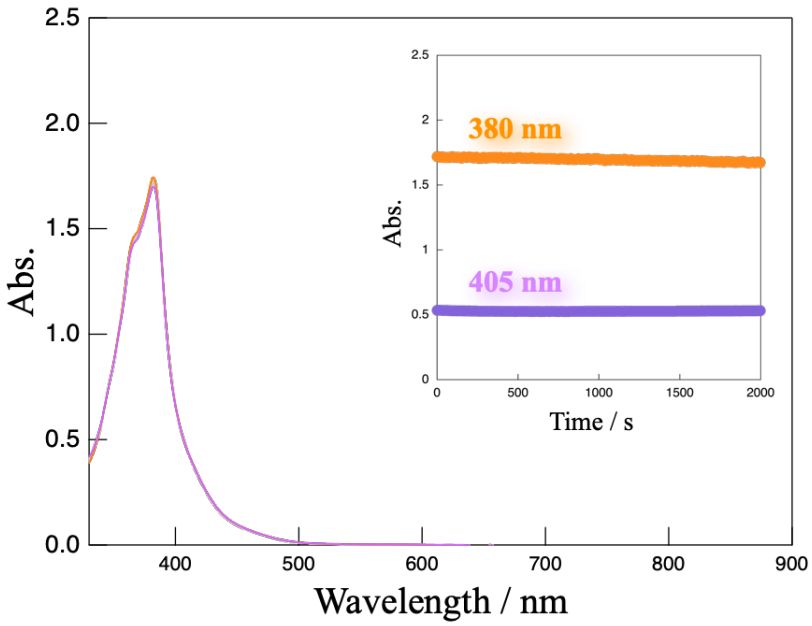

Fig. S13 Absorption spectral changes observed upon irradiation of the light (370 nm~) into the 0.05 mM CH_3CN solution of **1** in the presence of 3.0% v/v 1,1,1,3,3,3-hexafluoro-2-propanol at 298 K. Inset: Time course of the absorption change at 380 nm (orange circle) and 405 nm (purple circle).

References

1 W. L. F. Armarego and C. L. L. Chai, in *Purification of laboratory chemicals, 6th ed*., Pergamon Press, Oxford, 2009.

2 T.-a. Koizumi and K. Tanaka, *Angew. Chem., Int. Ed.,* 2005, **44,** 5891.

3 C. K. Mann and K. K. Barnes, in *Electrochemical reactions in non-aqueous systems*, Mercel Dekker, New York, 1970.

4 G. M. Sheldrick, *Acta Cryst*., 2015, **A71**, 3.

5 G. M. Sheldrick, *Acta Cryst*., 2015, **C71**, 3.